Methodology for reducing the filtering capacitor in low-flicker LED drivers

Ali Shagerdmootaab, Mehrdad Moallem

School of Mechatronic Systems Engineering, Simon Fraser University, Surrey, BC, Canada
E-mail: mmoallem@sfu.ca

Published in *The Journal of Engineering*; Received on 9th March 2017; Accepted on 27th April 2017

Abstract: The amount of light flicker in an AC–DC light-emitting diode (LED) driver is dependent on the size of filter capacitors. In this study, a study is conducted on reducing the size of filter capacitor in an AC–DC buck–boost/flyback LED driver using flicker index and per cent flicker light measures. Using this approach, a procedure for minimising the filter capacitance is presented. It is then concluded that relatively small filter capacitors such as film or ceramic capacitors can be chosen while meeting light flicker requirements. Hence, an LED drive with a longer lifetime can be achieved when compared with a driver using electrolytic capacitors. Experimental studies are presented for a 20 W AC–DC buck–boost/flyback LED driver prototype which utilises ceramic capacitors for driving Cree CR22-32L and XLamp XP-G LED strings.

1 Introduction

High-brightness light-emitting diodes (LEDs) have developed rapidly in recent years [1–4]. Among different attributes of light sources, constant and flicker-free output light is a desirable feature in their selection for lighting applications. Flicker from visible or invisible light sources can cause harmful neurological responses [5]. It has been shown that light source flicker can decrease the reading performance and cause annoyance for human body [6]. The Illuminating Engineering Society (IES) introduced flicker index and per cent flicker as two light flicker measures proposed by lighting designers [7], which is also proposed in the IEEE 1789TM-2015 standard [8].

A common LED driver usually consists of a single-stage AC–DC converter with power factor correction (PFC) [9, 10]. In a PFC LED driver, the input current and voltage are in phase with each other, leading to a pulsating input power for constant LED power. Hence, a large filter capacitor, e.g. normally an electrolytic capacitor, is required for power balance purposes [11]. The short lifetime of these types of capacitors, restricts the LED driver's lifetime.

Several techniques have been proposed to increase the lifetime of LED drivers. In [12], a pulsating current LED driver was presented in which the low-frequency component of LED current was reduced without using any electrolytic capacitors. In [13], the proposed converter is comprised of a rectifier-side storage capacitor along with a three-winding transformer to provide energy to the output LED string. The concept was utilised in [14], where a DC-link capacitor and coupled inductors were used to provide energy to the LED, resulting in low-ripple LED current with a small DC-link capacitor. Injection of the third harmonic into the input current, while meeting the EN61000-3-2 standard, was studied in [15] by which the size of filter capacitance was reduced. The method of injecting higher odd harmonics to the input current to reduce its peak-to-average ratio was studied in [16]. Although, injection of odd harmonics introduced in these studies reduces the filter capacitance, a main drawback is that the input power factor is sacrificed. In other approaches, utilisation of active storage capacitors instead of electrolytic capacitors to absorb the AC component of the pulsating input current was proposed [17, 18]. In [19], a new method was presented for incorporating the effect of light flicker and input current harmonics in the design of an AC–DC flyback LED driver to minimise the required filter capacitance. It was shown that by combining the maximum permissible light flicker, based on the ENERGY STAR standard, and injection of third and fifth harmonics to the input current, the required filter capacitance can be minimised. In [20], an integrated double buck–boost LED driver was proposed in which electrolytic capacitors were used.

The contribution of this paper is to provide a quantitative relationship between LED light flicker, the input current, and the filter capacitance in a buck–boost/flyback LED driver as shown in Fig. 1*a*. Integrated buck–boost/flyback converter compared with flyback converter studied in [19] leads to a much smaller filter capacitor due to the two stages topology. For the LED strings studied in [19], the size of filter capacitors were in the range of 100 μf while using the buck–boost/flyback converter they can be reduced to the range of 10 μf. Buck–boost topology at the input stage shows resistive input behaviour in the discontinuous conduction mode (DCM) through which a high-input power factor can be achieved. Furthermore, utilising the flyback topology in the output stage provides electrical isolation for safety issues. Using the above quantitative relationship, the filter capacitance can be determined for the whole range of permissible amplitudes of the LED light flicker while meeting the ENERGY STAR standard. The proposed method can thus be used to minimise the size of the required filter capacitors to the range of long-lifetime non-electrolytic capacitors.

This paper is organised as follows. In Section 2, the effect of LED light flicker and input current on the filter capacitance is studied. We present a quantitative relationship between the size of filter capacitors and the LED light flicker index, or per cent flicker measure. In Section 3, the above relationship is utilised to obtain the minimum filter capacitance. Experimental results are presented in Section 4 to show validity of the proposed method.

2 Analytic study of the proposed method

2.1 Input current effect on filter capacitor voltage

In this paper, the AC–DC buck–boost/flyback topology as shown in Fig. 1*a* [21] is considered when operating in the DCM. In this mode of operation, the circuit exhibits a *resistive* behaviour from the input leading to a high-input power factor. By denoting the input voltage source as $v_i(t) = V_m \sin \omega t$, the input current for input power factor of 1 is given as follows:

$$i_i(t) = I_m \sin \omega t \tag{1}$$

where V_m is the amplitude of the input voltage, I_m is the amplitude of the input current, and ω is the angular frequency of the input

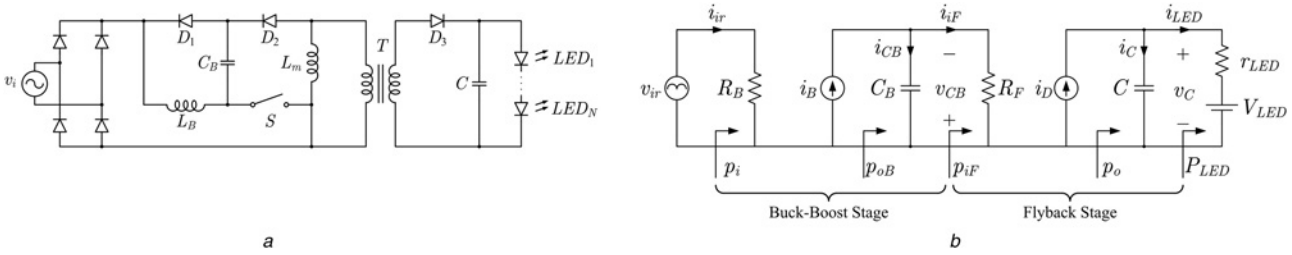

Fig. 1 *Quantitative relationship between LED light flicker, the input current, and the filter capacitance in a buck–boost/flyback LED driver*
a AC–DC buck–boost/flyback LED driver
b Its equivalent circuit

voltage. Utilising (1) and input voltage, the input power is given by

$$p_{\mathrm{i}}(t) = \frac{1}{2} V_{\mathrm{m}} I_{\mathrm{m}} (1 - \cos 2\omega t) \tag{2}$$

Fig. 1*b* shows the equivalent circuit of the LED driver as shown in Fig. 1*a*. In this figure, v_{ir} is the rectified voltage after diode bridge in Fig. 1*a*. The input power given by (2) is the power drawn from v_{ir} and delivered to the buck–boost equivalent resistance R_{B} given by [22]

$$R_{\mathrm{B}} = \frac{2L_{\mathrm{B}} f_{\mathrm{s}}}{D^2} \tag{3}$$

where L_{B} is the buck–boost stage inductor, f_{s} is the switching frequency, and D is the quiescent value of duty cycle of switch S. In the equivalent circuit, the output of the buck–boost converter is modelled as a current source i_{B} in parallel with the output filter capacitor C_{B}. By referring to Fig. 1*b* and assuming 100% efficiency for this stage, the power balance, i.e. $p_{\mathrm{oB}}(t) = p_{\mathrm{i}}(t)$, can be utilised to obtain the current source i_{B} as follows:

$$i_{\mathrm{B}}(t) = M_{\mathrm{B}}(t) i_{\mathrm{ir}}(t) \tag{4}$$

where $M_{\mathrm{B}}(t) = v_{\mathrm{ir}}(t)/v_{\mathrm{CB}}(t)$ and $i_{\mathrm{ir}}(t)$ is the rectified input current. Since the ripple of voltage $v_{\mathrm{ir}}(t)$ is much higher than the capacitor voltage variations, $M_{\mathrm{B}}(t)$ can be approximated using the average of $v_{\mathrm{CB}}(t)$, i.e. $M_{\mathrm{B}}(t) \simeq v_{\mathrm{ir}}(t)/V_{\mathrm{CB}}$. Therefore, (4) can be rewritten as follows:

$$i_{\mathrm{B}}(t) \simeq \frac{v_{\mathrm{ir}}(t)}{V_{\mathrm{CB}}} i_{\mathrm{ir}}(t) = \frac{p_{\mathrm{i}}(t)}{V_{\mathrm{CB}}} = I_b (1 - \cos 2\omega t) \tag{5}$$

where $I_{\mathrm{b}} = V_{\mathrm{m}} I_{\mathrm{m}} / 2V_{\mathrm{CB}}$. Utilising the equivalent circuit, the input of the flyback stage is modelled as a resistance given by

$$R_{\mathrm{F}} = \frac{2L_{\mathrm{m}} f_{\mathrm{s}}}{D^2} \tag{6}$$

where L_{m} is the magnetising inductance of the flyback transformer. To obtain the capacitor voltage v_{CB}, the following differential equation needs to be solved:

$$\frac{\mathrm{d}v_{\mathrm{CB}}(t)}{\mathrm{d}t} + \frac{1}{\tau_{\mathrm{B}}} v_{\mathrm{CB}}(t) = \frac{R_{\mathrm{F}}}{\tau_{\mathrm{B}}} i_{\mathrm{B}}(t) \tag{7}$$

where $\tau_{\mathrm{B}} = R_{\mathrm{F}} C_{\mathrm{B}}$. Solving (7) results in

$$v_{\mathrm{CB}}(t) = R_{\mathrm{F}} I_{\mathrm{b}} \left(1 - \frac{2\omega\tau_{\mathrm{B}} \sin 2\omega t + \cos 2\omega t}{1 + (2\omega\tau_{\mathrm{B}})^2}\right) + \exp_{\mathrm{decay}}(t) \tag{8}$$

where $\exp_{\mathrm{decay}}(t)$ is an exponentially decaying term. The time constant for the buck–boost stage is given by τ_{B} which is approximately in the order of milliseconds for $L_{\mathrm{m}} = 1\,\mathrm{mH}$, $C_{\mathrm{B}} = 10\,\mu\mathrm{F}$, small values of D in the DCM, and frequency in the range of kilohertz. Thus, the exponential term in (8) decays quickly to zero. Furthermore, using the above values we have $2\omega\tau_{\mathrm{B}} \gg 1$, from which (8) can be simplified as follows:

$$v_{\mathrm{CB}}(t) \simeq R_{\mathrm{F}} I_{\mathrm{b}} \left(1 - \frac{\sin 2\omega t}{2\omega\tau_{\mathrm{B}}}\right) + \exp_{\mathrm{decay}}(t) \tag{9}$$

Using (9) and assuming that the steady state is reached, i.e. the exponential term decays to zero, the input power to the flyback stage can be obtained as follows:

$$p_{\mathrm{iF}}(t) = \frac{v_{\mathrm{CB}}^2(t)}{R_{\mathrm{F}}} \simeq R_{\mathrm{F}} I_{\mathrm{b}}^2 \left(1 - \frac{\sin 2\omega t}{\omega\tau_{\mathrm{B}}}\right) \tag{10}$$

in which the second-order term is cancelled due to its small value. Using Fig. 1*b*, the current source i_{D} in the output of the flyback stage is in parallel with the output filter capacitor C. On the basis of Fig. 1*b* and assuming 100% efficiency for this stage, the power balance, i.e. $p_{\mathrm{o}}(t) = p_{\mathrm{iF}}(t)$, can be utilised to obtain the current source i_{D} as follows:

$$i_{\mathrm{D}}(t) = M_{\mathrm{F}}(t) i_{\mathrm{iF}}(t) \tag{11}$$

where $M_{\mathrm{F}}(t) = v_{\mathrm{CB}}(t)/v_{\mathrm{C}}(t)$ and $i_{\mathrm{iF}}(t)$ is the input current of the flyback stage. Since the ripple of voltage $v_{\mathrm{CB}}(t)$ is much higher than the ripple of voltage $v_{\mathrm{C}}(t)$, $M_{\mathrm{F}}(t)$ can be approximated using the average of voltage $v_{\mathrm{C}}(t)$, i.e. $M_{\mathrm{F}}(t) \simeq v_{\mathrm{CB}}(t)/V_{\mathrm{C}}$. Therefore, the current source i_{D} in (11) can be rewritten as follows:

$$i_{\mathrm{D}}(t) \simeq \frac{v_{\mathrm{CB}}(t)}{V_{\mathrm{C}}} i_{\mathrm{iF}}(t) = \frac{p_{\mathrm{iF}}(t)}{V_{\mathrm{C}}} = I_{\mathrm{d}} \left(1 - \frac{\sin 2\omega t}{\omega\tau_{\mathrm{B}}}\right) \tag{12}$$

where $I_{\mathrm{d}} = R_{\mathrm{F}} I_{\mathrm{b}}^2 / V_{\mathrm{C}}$. In the equivalent circuit given by Fig. 1*b*, the LED is modelled as V_{LED} in series with r_{LED} [23, 24]. To obtain the capacitor voltage $v_{\mathrm{C}}(t)$, the following differential equation needs to be solved:

$$\frac{\mathrm{d}v_{\mathrm{C}}(t)}{\mathrm{d}t} + \frac{1}{\tau_{\mathrm{F}}} v_{\mathrm{C}}(t) = \frac{r_{\mathrm{LED}}}{\tau_{\mathrm{F}}} i_{\mathrm{D}}(t) + \frac{1}{\tau_{\mathrm{F}}} V_{\mathrm{LED}} \tag{13}$$

where $\tau_{\mathrm{F}} = r_{\mathrm{LED}} C$. Solving (13) results in

$$v_{\mathrm{C}}(t) = V_{\mathrm{LED}} + r_{\mathrm{LED}} I_{\mathrm{d}} \left(1 + \frac{2\omega\tau_{\mathrm{F}} \cos 2\omega t - \sin 2\omega t}{\omega\tau_{\mathrm{B}}(1 + (2\omega\tau_{\mathrm{F}})^2)}\right) + \exp_{\mathrm{decay}}(t) \tag{14}$$

where $\exp_{\mathrm{decay}}(t)$ is an exponentially decaying term. Equation (14) represents the effect of the first harmonic of the input current on the output capacitor voltage and consequently the LED light flicker as

discussed in Section 2.2. From (13), the time constant $\tau_F \simeq 0.01$ ms for $r_{LED} = 1\ \Omega$ and $C = 10\ \mu F$ that results fast decay of the exponential part of $v_C(t)$ to zero.

2.2 Effect on output light flicker

According to the IES Lighting Handbook [7], flicker index, and per cent flicker have been proposed by lighting designers as two measures of light flicker. It was shown in [19] that, considering $v_C(t)$ across the LED string, the LED luminous flux is given by

$$\phi_v(t) = -\frac{\alpha_1 V_{LED}}{r_{LED}} v_C(t) + \left(\frac{\alpha_1}{r_{LED}} - \frac{\alpha_2 V_{LED}^2}{r_{LED}^2}\right) v_C^2(t) + \frac{2\alpha_2 V_{LED}}{r_{LED}^2} v_C^3(t) - \frac{\alpha_2}{r_{LED}^2} v_C^4(t) \quad (15)$$

where α_1 and α_2 are coefficients that can be obtained using the thermal characteristics of the LED and V_{LED} and r_{LED} are the electrical characteristics of the LED. Following [19], the flicker index and per cent flicker are given by:

$$\text{flicker index} = \frac{2f}{\phi_{vavg}} \int_{t_1}^{t_2} (\phi_v(t) - \phi_{vavg})\, dt \quad (16)$$

and

$$\text{percent flicker} = \frac{\phi_{vmax} - \phi_{vmin}}{\phi_{vmax} + \phi_{vmin}} \times 100 \quad (17)$$

where ϕ_{vmin}, ϕ_{vavg}, and ϕ_{vmax} are the minimum, average, and maximum LED luminous flux, respectively; $f = 1/T$ is the fundamental frequency; and t_1 and t_2 are time instants depicted in Fig. 2*a*. The LED output luminous flux in (15) is independent of the converter's topology and is applicable to all PFC converters. It depends on the instantaneous LED voltage and its electrical and photometric characteristics.

Accurate measurement of luminous flux ϕ_v is required for photometric flicker analysis. Instead, the illuminance E_v can be measured using an ambient light sensor as shown in Fig. 2*b*, where $E_v = k\phi_v$ and k is a coefficient representing the portion of the LED luminous flux that illuminates the surface of the sensor. The accuracy of this procedure was proven in [19] that is also used in this paper.

A numerical procedure utilising (16) and (17) will be discussed in Section 3 to obtain the filter capacitances C and C_B. In [25], a combination of flicker index and per cent flicker measures are referred to as flicker frame of reference. Referring to the ENERGY STAR standard, most light sources are enclosed in this frame by a maximum flicker index and per cent flicker of 0.13 and 40%, respectively.

To meet the ENERGY STAR standard for the LED light flicker, capacitor degradation effect has to be considered that results in the LED light flicker increase. In the proposed control algorithm, the input current is controlled to follow the same phase of the input voltage for achieving high-power factor. Thus, filter capacitor degradation does not affect the input power factor. The capacitor degradation coefficient has to be considered in the filter capacitance minimisation algorithm. Note that, by establishing a relationship between input current and capacitor voltage the same as (14) for other LED driver structures, the proposed method can be used to minimise the filter capacitance.

3 Filter capacitance minimisation

3.1 LED strings characterisation

In this paper, Cree CR22-32L and XLamp XP-G LED strings were selected for experimental evaluation. To obtain the minimum required filter capacitances based on different LED powers and light flickers [i.e. solving (16) and (17)], r_{LED}, V_{LED}, α_1, and α_2 referred to as the electrical and photometric characteristics of these LED strings need to be obtained. The procedure for obtaining these parameters was presented in [19]. On the basis of that study, the LED current, internal resistance, and power are modelled, respectively, as follows:

$$i_{LED} = \begin{cases} 0 & v_C \le V_{LED} \\ a e^{b(v_C - V_{LED})} & v_C > V_{LED} \end{cases} \quad (18)$$

$$r_{LED} = \left(\frac{di_{LED}}{dv_C}\right)^{-1} = \frac{1}{ab} e^{-b(v_C - V_{LED})} \quad (19)$$

and

$$p_{LED} = a v_C e^{b(v_C - V_{LED})} \quad (20)$$

Fig. 3*a* shows the measured LED current i_{LED} versus LED voltage v_C higher than 25 V for CR22-32L LED string. By applying regression analysis to this plot, the LED current given by (18) was obtained with $V_{LED} = 25$ V, $a = 0.04$, and $b = 0.54$. The same procedure was followed for XLamp XP-G LED and $V_{LED} = 35$ V, $a = 0.012$, and $b = 0.57$ were obtained. For photometric characteristics, the output illuminance E_v versus LED power P_{LED} was plotted in Fig. 3*b*. Using regression analysis and

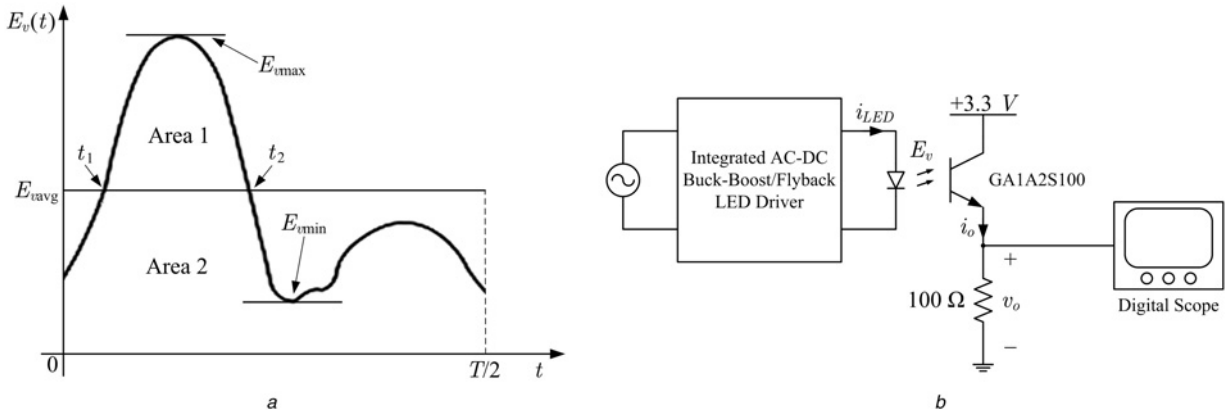

Fig. 2 *Effect on output light flicker*
a Illuminance of LED light to define flicker index and per cent flicker
b Ambient light sensor circuitry for flicker measurement

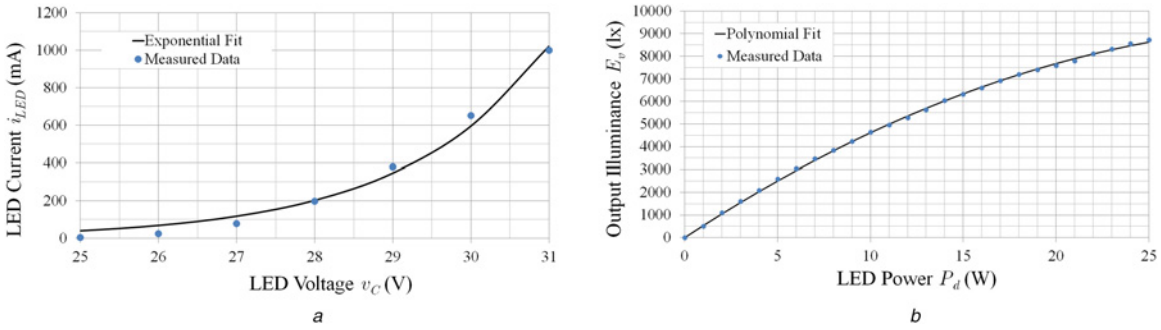

Fig. 3 *LED strings characterisation*
a Measured LED current versus LED voltage data for CR22-32L LED and its exponential fit
b Measured LED illuminance versus LED power data for CR22-32L LED and its polynomial fit

LED datasheet, $\alpha_1 = 100\,\text{lum/W}$ and $\alpha_2 \simeq 1.44\,\text{lum/W}^2$ were obtained. For the XLamp XP-G LED string, $\alpha_1 = 94\,\text{lum/W}$ and $\alpha_2 \simeq 1.84\,\text{lum/W}^2$ were obtained.

3.2 Filter capacitance minimisation algorithm

Assume that the filter capacitors C and C_B have to be determined. Thus, v_C in (14) is a function of time t and filter capacitances, i.e. $v_C(t,\ C,\ C_B)$. Consequently, ϕ_v in (15) has the same dependency to time and filter capacitances, i.e. $\phi_v(t,\ C,\ C_B)$. As a result, (16) can be rewritten as follows:

$$\text{flicker index} = \frac{2f}{\phi_{v\text{avg}}}\int_{t_1}^{t_2}(\phi_v(t,\ C,\ C_B) - \phi_{v\text{avg}})\,\mathrm{d}t \qquad (21)$$

For a given LED applied power, the effect of filter capacitors on the light flicker can be studied by utilising (17) and (21) with the following numerical procedure:

(i) Obtain $\phi_v(t,\ C,\ C_B)$ from (15) with known parameters, i.e. f, r_{LED}, V_{LED}, α_1, α_2, P_d, L_m, and L_B.
(ii) Obtain $\phi_v(t)$ by substituting a known C and C_B.
(iii) Calculate $\phi_{v\text{min}}$, $\phi_{v\text{avg}}$, and $\phi_{v\text{max}}$.
(iv) Calculate t_1 and t_2 by obtaining roots of $\phi_v(t) - \phi_{v\text{avg}}$.
(v) Calculate flicker index and per cent flicker using (21) and (17), respectively.

The above algorithm was used for C and $C_B = 10, 20, 30, 40$, and $50\,\mu\text{F}$ when $P_d = 10\,\text{W}$ for CR22-32L LED. The results are shown in Tables 1 and 2 for flicker index and per cent flicker, respectively. At each power operating point, $v_C(t)$ can be obtained utilising (20), which is then used in (19) to obtain the LED resistance r_{LED} for the minimisation algorithm. In Table 1, the flicker index is below 0.13 which is the maximum permissible for any capacitors in the table for both C and C_B. Also, in Table 2, the per cent flicker is below the maximum permissible, i.e. 40%, with the same capacitors and LED power. These results show that a larger filter capacitor leads to a lower light flicker as expected.

The same procedure was followed for $P_d = 20\,\text{W}$ with the results as shown in Tables 3 and 4 for flicker index and per cent flicker, respectively. These results also show that, with higher LED power, the light flicker is higher using the same filter capacitors. Hence, by choosing the highest LED power as the operating point and obtaining its minimum required capacitor, the LED light flicker requirements for lower-power levels is satisfied.

Table 1 Flicker index for CR22-32L LED with different C and C_B and $P_d = 10\,\text{W}$

C, μF	C_B				
	10 μF	20 μF	30 μF	40 μF	50 μF
10	0.12	0.12	0.12	0.11	0.11
20	0.12	0.12	0.11	0.11	0.11
30	0.12	0.11	0.11	0.11	0.10
40	0.11	0.10	0.10	0.10	0.09
50	0.11	0.10	0.10	0.09	0.09

Table 2 Per cent flicker (%) for CR22-32L LED with different C and C_B and $P_d = 10\,\text{W}$

C, μF	C_B				
	10 μF	20 μF	30 μF	40 μF	50 μF
10	34	30	27	25	23
20	32	29	27	24	22
30	30	27	25	23	21
40	28	26	24	23	21
50	26	24	23	22	20

Table 3 Flicker index for CR22-32L LED with different C and C_B and $P_d = 20\,\text{W}$

C, μF	C_B				
	10 μF	20 μF	30 μF	40 μF	50 μF
10	0.14	0.14	0.13	0.13	0.13
20	0.14	0.13	0.13	0.12	0.11
30	0.13	0.12	0.12	0.11	0.11
40	0.12	0.12	0.11	0.11	0.11
50	0.12	0.11	0.11	0.11	0.10

Table 4 Per cent flicker (%) for CR22-32L LED with different C and C_B and $P_d = 20\,\text{W}$

C, μF	C_B				
	10 μF	20 μF	30 μF	40 μF	50 μF
10	37	33	30	27	25
20	35	32	29	26	24
30	33	30	28	25	23
40	31	29	27	25	23
50	29	27	25	24	22

As shown in Table 3, by using smaller filter capacitances, the flicker index reaches above the maximum permissible value. In Table 4, the per cent flicker is below the maximum permissible value for all capacitors specified. To meet the light flicker standard, the filter capacitors by which both flicker index and per cent flicker reach their maximum permissible values can be selected to be the minimum required capacitor. On the basis of these results, $C = 20\,\mu F$ and $C_B = 20\,\mu F$ are the smallest filter capacitors that are required to meet light flicker requirements. Thus, long-lasting film or ceramic capacitors can be used.

The same calculation was done for C and $C_B = 10$, 20, 30, 40, and 50 μF, when $P_d = 10$ and 20 W for an XLamp XP-G LED. The results for $P_d = 10$ W are shown in Tables 5 and 6 for flicker index and per cent flicker, respectively. In these tables, both flicker index and per cent flicker are below the maximum permissible values. For $P_d = 20$ W, the results are shown in Tables 7 and 8 for flicker index and per cent flicker, respectively. Thus, the flicker index and per cent flicker are below the maximum permissible values for all capacitors in the table for both C and C_B. These results show that for higher powers, both flicker index and per cent flicker are higher. Therefore, choosing the minimum required capacitor, i.e. 10 μF, based on the higher power would guarantee that light flicker measures are satisfied for lower-power levels.

Table 5 Flicker index for XLamp XP-G LED with different C and C_B and $P_d = 10$ W

C, μF	C_B				
	10 μF	20 μF	30 μF	40 μF	50 μF
10	0.11	0.11	0.10	0.10	0.09
20	0.11	0.11	0.10	0.09	0.09
30	0.10	0.10	0.09	0.09	0.08
40	0.10	0.09	0.09	0.08	0.08
50	0.09	0.09	0.08	0.08	0.07

Table 6 Per cent flicker (%) for XLamp XP-G LED with different C and C_B and $P_d = 10$ W

C, μF	C_B				
	10 μF	20 μF	30 μF	40 μF	50 μF
10	27	24	22	20	18
20	25	23	20	18	16
30	23	20	18	17	15
40	21	19	17	15	14
50	19	17	16	14	13

Table 7 Flicker index for XLamp XP-G LED with different C and C_B and $P_d = 20$ W

C, μF	C_B				
	10 μF	20 μF	30 μF	40 μF	50 μF
10	0.13	0.13	0.12	0.11	0.11
20	0.13	0.12	0.12	0.11	0.10
30	0.12	0.12	0.11	0.10	0.10
40	0.11	0.11	0.10	0.09	0.09
50	0.10	0.10	0.09	0.09	0.08

Table 8 Per cent flicker (%) for XLamp XP-G LED with different C and C_B and $P_d = 20$ W

C, μF	C_B				
	10 μF	20 μF	30 μF	40 μF	50 μF
10	31	29	28	26	24
20	29	28	26	24	23
30	27	25	23	22	21
40	26	24	22	21	20
50	24	22	21	19	18

A simulation study was performed to drive XLamp XP-G LED string under different loads. The capacitor voltages v_{CB} and v_C were plotted in Figs. 4*a* and *b* for 10 and 20 W LED powers, respectively. This figure shows that voltage ripple on both capacitors are higher for higher loads that results in higher flicker index and per cent flicker. It is in agreement with the results in Tables 5 and 7 that flicker index is higher for higher LED power. Also, it is in agreement with the results in Tables 6 and 8 for per cent flicker.

3.3 *Input current control algorithm*

On the basis of the discussion in Section 3, if the input current of the converter contains only the first harmonic, then the requirements for ENERGY STAR measures can be met using small filter capacitors. Fig. 5 shows the schematic diagram of the AC–DC buck–boost/flyback LED driver studied in this paper. In [26], the LED power control concept was studied by controlling the peak of the input current. It was shown that to achieve high-input power factor, the angular frequency of the input current can be kept in phase with the input voltage. Fig. 6*a* shows the block diagram to construct the desired input current and the input current control loop. Utilising (2), and assuming 100% converter efficiency, the desired LED power is given by

$$P_d = \frac{2}{T}\int_0^{T/2} p_i(t)\,dt = \frac{V_m I_m}{2} \tag{22}$$

As shown in Fig. 6*a*, the amplitude of the desired input current is constructed using P_d and V_m by using (22). Also, the angular frequency for the desired input current is constructed using the normalised input voltage fed into a lookup table. The desired input current $|i_{id}|$ is utilised to control the input current of the converter. By changing the desired power P_d, the amplitude of the desired input current I_m will change. This results in LED dimming without sacrificing input power factor.

4 Experimental results

A 20 W prototype of the power circuitry that was tested under 120 V_{rms} is shown in Fig. 6*b*. In this paper, buck–boost converter was selected as the input stage of the converter due to its similarity to flyback converter. It helps to use the same cascade control method in [26] to control the input current and LED power. The buck–boost topology operating in DCM provides high-power factor and low total harmonic distortion (THD) when the input current and voltage are in phase with each other. The LED power is regulated by controlling the input current of the buck–boost converter in the primary side. The input power factor depends on the input current control method. Thus, any changes in the capacitances C and C_B do not have any effect on the input power factor and THD and only affects the LED light flicker.

Any input line voltage variations does not affect the input power factor and THD. It is because the input current is controlled to follow the desired input current in phase with input voltage.

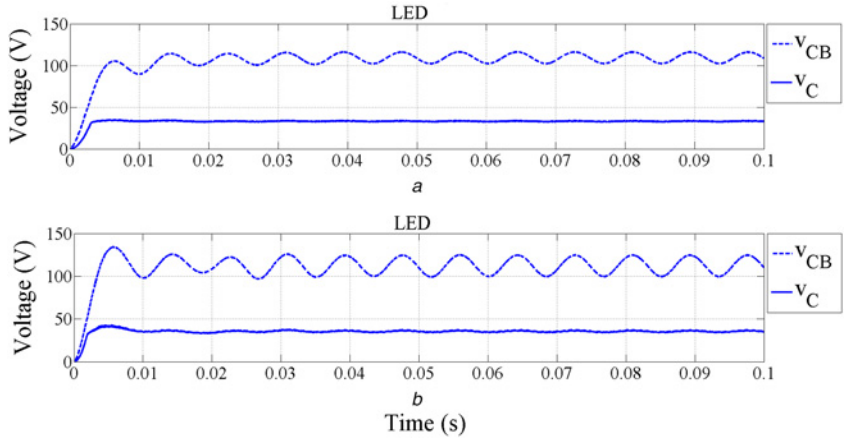

Fig. 4 *Voltages of the two capacitors C and C_B at*
a 10 W
b 20 W LED powers

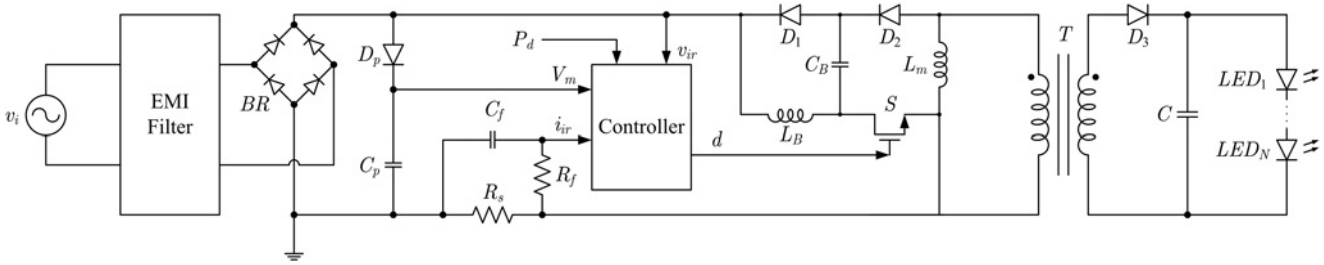

Fig. 5 *Schematic circuit of the integrated buck–boost/flyback LED driver with LED power and input current controllers diagram*

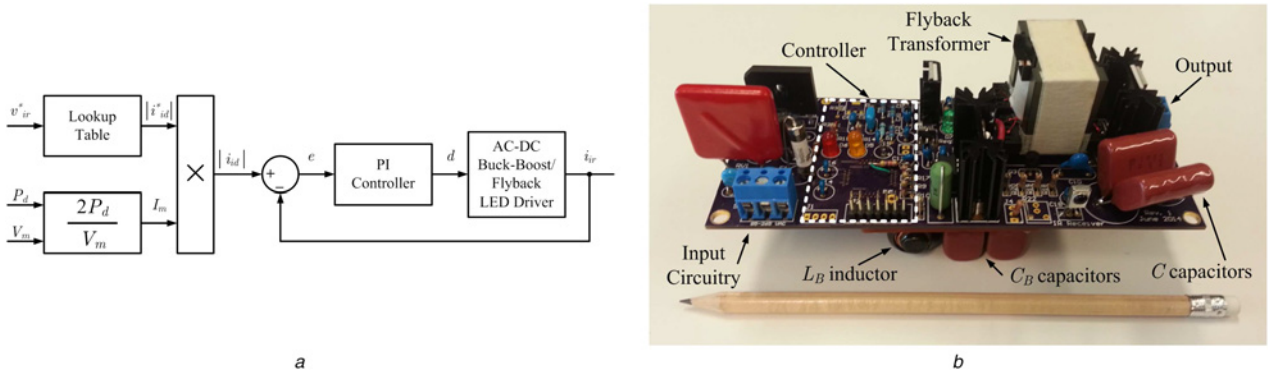

Fig. 6 *Block diagram to construct the desired input current and the input current control loop*
a Schematic representation of the buck–boost/flyback LED driver
b Prototype of the LED driver

However, these variations will affect the voltages of filter capacitors, i.e. v_{CB} and v_C and consequently flicker index and per cent flicker. Any increase on input voltage line will increase the voltage ripple of filter capacitors and light flicker that has to be considered for minimisation algorithm in Section 3.2.

The controller implementation was achieved using a TMS320F28027 MCU from Texas Instruments. The components and power devices of the converter are as follows:

(i) *BR*: KBL10 (1000 V, 4 A);
(ii) D_1, D_2, and D_3: UF5408 (1000 V, 3 A);
(iii) *S*: IRFB11N50A (500 V, 11 A); and
(iv) *T*: 1207 μH primary inductance and 50/14 turns ratio.

On the basis of the results obtained in Section 3, two 20 μF capacitors with 50 and 250 V voltage ratings were used for *C* and C_B, respectively, in the power driver circuitry to drive Cree CR22-32L LED string. In this way, the flicker index and per cent flicker for 10 and 20 W were measured every 5 min during 1 h of operation of the circuit and plotted in Figs. 7*a* and *b*, respectively. Fig. 7*a* shows that for a power of 10 W, the flicker index is about 0.11 and the per cent flicker is about 27%, which are in good agreement with the results in Section 3.2 and meet the ENERGY STAR standard. Also, Fig. 7*b* shows that for a power of 20 W, the flicker index and per cent flicker are ~0.12 and 30%, respectively, which are again in good agreement with numerical results in Section 3.2.

The same tests were performed on a Cree XLamp XP-G LED string with two 10 μF capacitors with 50 and 250 V voltage ratings

doi: 10.1049/joe.2017.0092

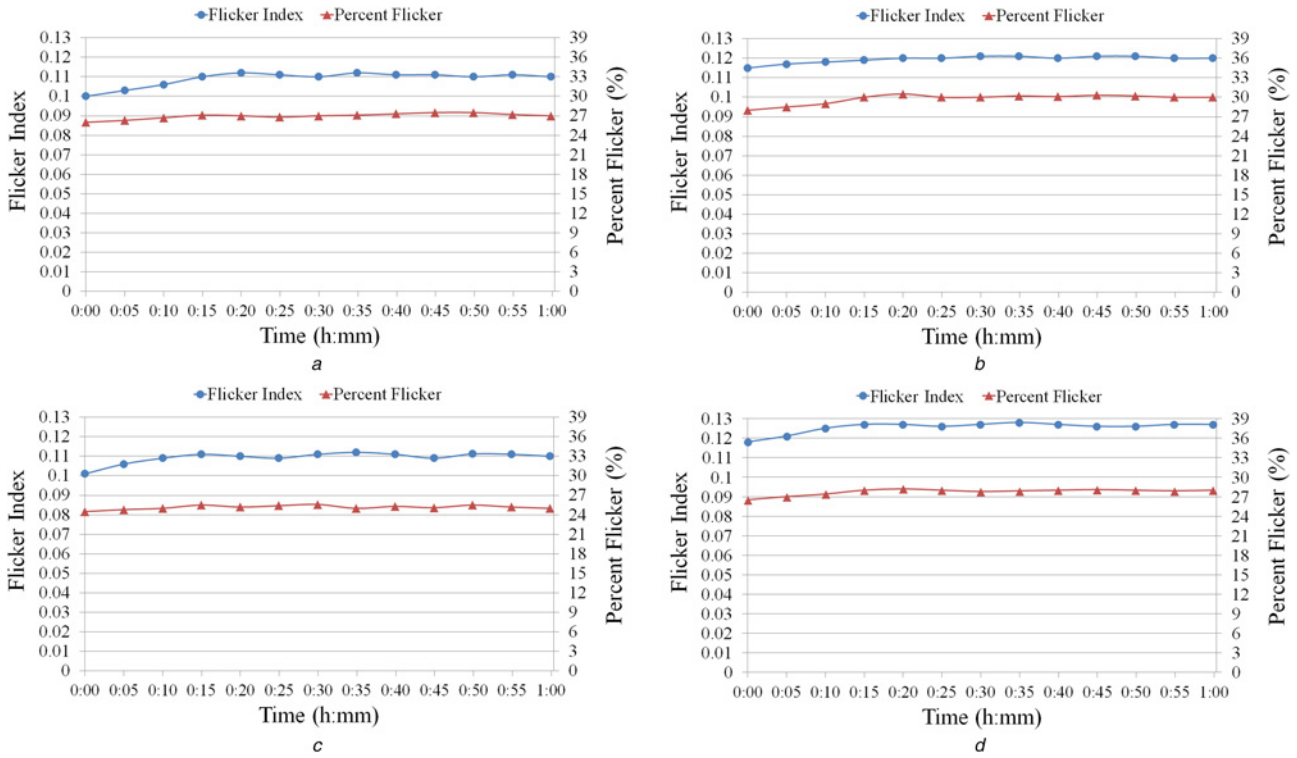

Fig. 7 *Flicker index and per cent flicker (%) of experimental setup for*
a CR22-32L LED string when $C = 20\,\mu F$, $C_B = 20\,\mu F$, and $P_d = 10\,W$
b CR22-32L LED string when $C = 20\,\mu F$, $C_B = 20\,\mu F$, and $P_d = 20\,W$
c XLamp XP-G LED string when $C = 10\,\mu F$, $C_B = 10\,\mu F$, and $P_d = 10\,W$
d XLamp XP-G LED string when $C = 10\,\mu F$, $C_B = 10\,\mu F$, and $P_d = 20\,W$

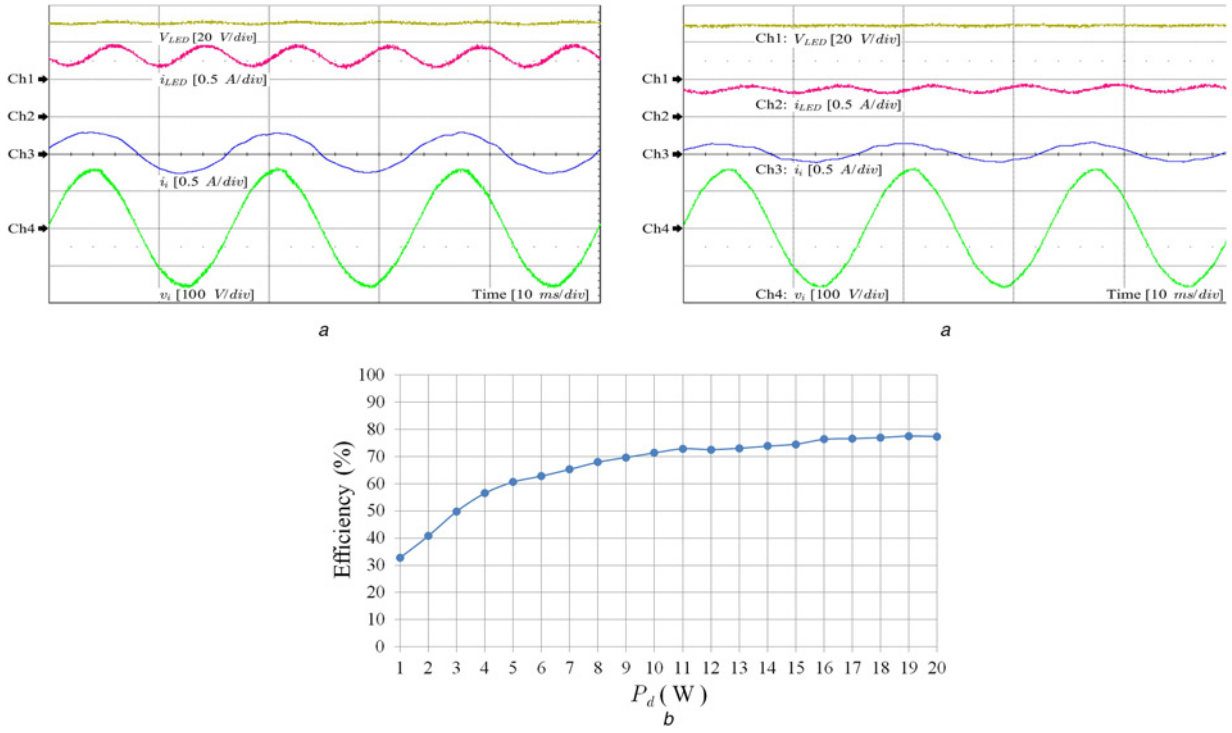

Fig. 8 *Waveforms of LED voltage (Ch1), LED current (Ch2), input current (Ch3), and input voltage (Ch4) of buck–boost/flyback LED driver with*
a $P_d = 10\,W$
b $P_d = 20\,W$ for CR22-32 LED string
c Efficiency of the converter with different LED powers under 120 V input voltage

doi: 10.1049/joe.2017.0092

used for C and C_B in the power drive circuitry as discussed in Section 3.2. The flicker index and per cent flicker were measured for 10 and 20 W and the results were updated every 5 min during 1 h of operation of the circuit as shown in Figs. 7*c* and *d*, respectively. These figures show that for a power of 20 W, the flicker index and per cent flicker are ~0.13 and 28%, respectively, which are in good agreement with the numerical results obtained in Section 3.2. Also, the light flicker for 10 W is lower than for 20 W as shown in Fig. 7*c*.

Fig. 8*a* presents the current and voltage waveforms of input and output of the AC–DC buck–boost/flyback LED driver when Cree CR22-32L LED string was connected to the output of the driver. For the controller, the input current control method proposed in [26] was utilised. As shown in this figure, the input current and voltage are almost in phase with each other that results power factor of almost 0.96. This figure also shows the output current and voltage waveforms of the driver when LED power is 20 W. The measured current and voltage ripple factors are 7.9 and 37.2%, respectively. Fig. 8*b* shows the same waveforms when LED power is 10 W. The measured current and voltage ripple factors are 6.2 and 34.9%, respectively. Fig. 8*c* shows the efficiency of the converter under 120 V input voltage for different LED powers ranges 1–20 W. It shows that for higher LED powers, the converter is more efficient.

On the basis of accelerated life tests on two high brightness light emitting diodes (HBLEDs) in [27], the series resistance of the LED can increase due to contact property worsening and detachment. Whereas ageing mechanisms in the LED's characteristics presented in [28] do not indicate major changes in the LED I–V curve for currents >1 mA. As a result, the series resistance of the LED can either increase or remain constant due to ageing. This means, the time constant of the second stage, i.e. flyback as shown in Fig. 1*b*, can increase or remain constant. Hence, the result would be reduction of the LED current and consequently light illuminance.

5 Conclusion

In this work, an algorithm was proposed for minimising the size of filter capacitors for an AC–DC buck–boost/flyback LED drive circuitry based on ENERGY STAR's flicker index and per cent flicker light flicker measures. A relationship between filter capacitors and these measures was obtained utilising small signal model of the converter. Furthermore, a numerical procedure was presented to obtain the light flicker measure using circuit and LED parameters with different filter capacitors. The results indicate that relatively small capacitors can be obtained while meeting requirements such as small light flicker and high-power factor. Hence, long-lifetime technologies such as film or ceramic capacitors can be used. A 20 W electrolytic capacitor-less LED driver was developed and its performance was verified experimentally to validate the proposed filter capacitor minimisation algorithm.

6 Acknowledgment

This research was supported by the Natural Sciences and Engineering Research Council of Canada.

7 References

[1] Chiu C., Chen K.: 'A high accuracy current-balanced control technique for LED backlight'. Proc. IEEE Power Electronics Specialists Conf. (PESC), 2008, pp. 4202–4206
[2] Qu X., Wong S.-C., Tse C.K.: 'Resonance-assisted buck converter for offline driving of power LED replacement lamps', *IEEE Trans. Power Electron.*, 2011, **26**, (2), pp. 532–540
[3] Chen N., Chung H.-H.: 'A driving technology for retrofit LED lamp for fluorescent lighting fixtures with electronic ballasts', *IEEE Trans. Power Electron.*, 2011, **26**, (2), pp. 588–601
[4] Hui S., Li S.N., Tao X.H., *ET AL.*: 'A novel passive offline LED driver with long lifetime', *IEEE Trans. Power Electron.*, 2010, **25**, (10), pp. 2665–2672
[5] Wilkins A., Veitch J., Lehman B.: 'LED lighting flicker and potential health concerns: IEEE standard PAR1789 update'. Energy Conversion Congress and Exposition (ECCE), 2010, pp. 171–178
[6] Lehman B., Wilkins A.: 'Biological effects and health hazards from flicker that is too rapid to see', 2010
[7] Kaufman J.E., Haynes H.: 'IES lighting handbook; reference volume and application volume', 1981
[8] IEEE: 'Recommended practices for modulating current in high-brightness LEDs for mitigating health risks to viewers', 2015
[9] Li Y.-C., Chen C.-L.: 'A novel single-stage high-power-factor AC-to-DC LED driving circuit with leakage inductance energy recycling', *IEEE Trans. Ind. Electron.*, 2012, **59**, (2), pp. 793–802
[10] Gacio D., Alonso J.M., Garcia J., *ET AL.*: 'PWM series dimming for slow-dynamics HPF LED drivers: the high-frequency approach', *IEEE Trans. Ind. Electron.*, 2012, **59**, (4), pp. 1717–1727
[11] Chiu H., Lo Y., Chen J., *ET AL.*: 'A high-efficiency dimmable LED driver for low-power lighting applications', *IEEE Trans. Ind. Electron.*, 2010, **57**, (2), pp. 735–743
[12] Lam J.C., Jain P.K.: 'A high power factor, electrolytic capacitor-less ac-input LED driver topology with high frequency pulsating output current', *IEEE Trans. Power Electron.*, 2015, **30**, (2), pp. 943–955
[13] Lam J., Jain P.K.: 'A novel isolated electrolytic capacitor-less single-switch AC–DC offline LED driver with power factor correction'. 29th Annual Meeting of IEEE Applied Power Electronics Conf. and Exposition (APEC), 2014, 2014, pp. 1356–1361
[14] Jain P.K., Lam J.: 'High power factor, electrolytic capacitor-less driver circuit for light-emitting diode lamps'. US Patent Application 14/219,692, 19 March 2014
[15] Gu L., Ruan X., Xu M., *ET AL.*: 'Means of eliminating electrolytic capacitor in AC–DC power supplies for LED lightings', *IEEE Trans. Power Electron.*, 2009, **24**, (5), pp. 1399–1408
[16] Wang B., Ruan X., Yao K., *ET AL.*: 'A method of reducing the peak-to-average ratio of LED current for electrolytic capacitor-less AC–DC drivers', *IEEE Trans. Power Electron.*, 2010, **25**, (3), pp. 592–601
[17] Wang S., Ruan X., Yao K., *ET AL.*: 'A flicker-free electrolytic capacitor-less AC–DC LED driver', *IEEE Trans. Power Electron.*, 2012, **27**, (11), pp. 4540–4548
[18] Yang Y., Ruan X., Zhang L., *ET AL.*: 'Feed-forward scheme for an electrolytic capacitor-less AC/DC LED driver to reduce output current ripple', *IEEE Trans. Power Electron.*, 2014, **29**, (10), pp. 5508–5517
[19] Shagerdmootaab A., Moallem M.: 'Filter capacitor minimization in a flyback LED driver considering input current harmonics and light flicker characteristics', *IEEE Trans. Power Electron.*, 2015, **30**, (8), pp. 4467–4476
[20] Alonso J.M., Viña J., Vaquero D.G., *ET AL.*: 'Analysis and design of the integrated double buck–boost converter as a high-power-factor driver for power-LED lamps', *IEEE Trans. Ind. Electron.*, 2012, **59**, (4), pp. 1689–1697
[21] Luz P., Cosetin M., Bolzan P., *ET AL.*: 'An integrated insulated buck–flyback converter to feed LED's lamps to street lighting with reduced capacitances'. IEEE Int. Conf. on Industrial Technology, 2015, pp. 908–913
[22] Alonso J., Dalla Costa M., Ordiz C.: 'Integrated buck–flyback converter as a high-power-factor off-line power supply', *IEEE Trans. Ind. Electron.*, 2008, **55**, (3), pp. 1090–1100
[23] Lin R.-L., Chen Y.-F.: 'Equivalent circuit model of light-emitting-diode for system analyses of lighting drivers'. Industry Applications Society Annual Meeting, 2009 IAS 2009, 2009, pp. 1–5
[24] Gacio D., Alonso J., Calleja A., *ET AL.*: 'A universal-input single-stage high-power-factor power supply for HB-LEDs based on integrated buck–flyback converter', *IEEE Trans. Ind. Electron.*, 2011, **58**, (2), pp. 589–599
[25] Lehman B., Wilkins A., Berman S., *ET AL.*: 'Proposing measures of flicker in the low frequencies for lighting applications'. 2011 IEEE Energy Conversion Congress and Exposition (ECCE), 2011, pp. 2865–2872
[26] Shagerdmootaab A., Moallem M.: 'A double-loop primary-side control structure for HB-LED power regulation', *IEEE Trans. Power Electron.*, 2016, **31**, (3), pp. 2476–2484
[27] Trevisanello L., Meneghini M., Mura G., *ET AL.*: 'Accelerated life test of high brightness light emitting diodes', *IEEE Trans. Device Mater. Reliab.*, 2008, **8**, (2), pp. 304–311
[28] Pursiainen O., Linder N., Jaeger A., *ET AL.*: 'Identification of aging mechanisms in the optical and electrical characteristics of light-emitting diodes', *Appl. Phys. Lett.*, 2001, **79**, (18), pp. 2895–2897